resemble the $\Gamma(\frac{3}{2})$ excitons; in particular, the binding energies should be much more nearly equal than in the solid films. In order to test this point it is necessary that for the $\Gamma(\frac{1}{2})$ excitons either $2s$ or plateau edge (series limit) be resolved in the liquid. From the unannealed spectrum this seems feasible. If the predicted similarity of the $\Gamma(\frac{1}{2})$ series to the $\Gamma(\frac{3}{2})$ series in the liquid is found experimentally, it will provide strong support for our over-all viewpoint.

ACKNOWLEDGMENTS

It is a pleasure to thank G. Baldini for stimulating discussions, and W. B. Fowler for stimulating correspondence.

PHYSICAL REVIEW VOLUME 136, NUMBER 6A 14 DECEMBER 1964

Ultraviolet Absorption of Insulators. V. The Cesium Halides*

J. C. PHILLIPS†
Department of Physics and Institute for the Study of Metals, University of Chicago, Chicago, Illinois
(Received 22 April 1964)

The intrinsic ultraviolet spectra of the simple cubic Cs halides measured by Eby, Teegarden, and Dutton are analyzed into exciton and scattering parts. The effects of configuration interaction on spin-orbit splittings are discussed semiquantitatively, and specific mechanisms are proposed. It is shown that the conduction bands can be separated into a lowest s-like band and higher d-like bands in CsCl and CsBr. In CsI the bands may overlap. The stability of the extra excitons appears to be reduced by configuration interaction in CsI.

1. INTRODUCTION

THIS paper continues the analysis of ultraviolet absorption in insulators previously carried out for tetrahedrally coordinated semiconductors,[1,2] fcc alkali halides,[3] and solid rare gases.[4] Our analysis of the Cs halides is somewhat less complete than previously. The reasons for this are:

(1) The spin-orbit splitting which was so useful for other insulators is less helpful here. In the other insulators the spin-orbit splitting of valence p states followed closely the atomic splittings, while the conduction band splittings were negligible. In the Cs halides, as discussed in Sec. 2, the valence splittings are anomalous.

(2) No complete band calculations are available for the conduction bands of the Cs halides. This difficulty also limited our work on fcc alkali halides, but there we were able to take advantage of band studies[5] of fcc Ar. It turned out that d bands play an important role, which we expect to be even larger in the Cs halides in accordance with the trends of alkali metals. The valence and conduction bands are constructed schematically in Secs. 3 and 4. The uv spectra are analyzed into exciton and scattering parts in Secs. 5 and 6.

2. SPIN-ORBIT SPLITTINGS

In the predominantly covalent group IV and III–V semiconductors the spin-orbit splitting of the valence band at $\mathbf{k}=0$ can be represented as the one-electron average of the splittings on the two atoms in the unit cell. In the III–V compounds the "neutral atom" average

$$\bar{\lambda}=0.35\lambda_{III}+0.65\lambda_V \qquad (2.1)$$

yields good agreement with experiment[6] over a range of λ_{III}/λ_V ratios from 0.03 to 5.4.

In predominantly ionic crystals it has been known for some time that there are systematic deviations from free-atom splittings.[7] These are usually lumped together under the heading of configuration interaction. The early data on substitutional Tl and Pb impurities in the alkali halides have been reviewed by Knox.[8] He mentions a number of possible configuration interactions without specifically favoring any. As an introduction to the subject of spin-orbit splittings in predominantly ionic crystals, we review the data on substitutional Tl splittings in fcc alkali halides and suggest that it can be understood in terms of three specific effects. The data are shown in Table I.

The free ion splitting of Tl^+ is 1.25 eV. In general, the spin-orbit splitting in the crystal tends to be larger than in the free atom or ion because of compression of

* Supported in part by the National Science Foundation, the U. S. Office of Naval Research, and a general grant to the ISM by ARPA.
† Alfred P. Sloan Fellow.
[1] J. C. Phillips, Phys. Rev. **125**, 1931 (1962).
[2] J. C. Phillips, Phys. Rev. **133**, A452 (1964).
[3] J. C. Phillips, Phys. Rev. **136**, A1705 (1964), Paper III, this issue.
[4] J. C. Phillips, Phys. Rev. **136**, A1714 (1964), Paper IV, this issue.
[5] L. F. Mattheiss, Phys. Rev. **133**, A1399 (1964).
[6] M. Cardona, J. Appl. Phys. **32**, 2151S (1961); L. Liu, Phys. Rev. **126**, 1321 (1962).
[7] J. E. Eby, K. J. Teegarden, and D. B. Dutton, Phys. Rev. **116**, 1099 (1959); referred to as ETD.
[8] R. S. Knox, Phys. Rev. **115**, 1095 (1959).

TABLE I. The spin-orbit splittings of the $6s6p$ state of Tl^+ impurities in fcc alkali halide crystals. The experimental values from phosphor spectra are taken from Knox (Ref. 8). The average theoretical values for each halide group are calculated using (2.2) and (2.3) and the assumed values of β^2 shown in the table. The trends within each halide group are discussed in the text.

Host crystal	Δ_{s0}(exptl) eV	β^2	Δ_{s0}(theory) $=\bar{\lambda}$ eV
Chlorides			
NaCl	1.33		
KCl	1.37	0.25	1.35
RbCl	1.42		
Bromides			
NaBr	1.09		
KBr	1.15	0.30	1.17
RbBr	1.05		
Iodides			
NaI	1.06		
KI	0.93	0.35	0.89
RbI	0.82		

the charge density (change of normalization) in the crystal. The splitting in crystalline Ge, e.g., is the same[6] as in the free *ion* Ge^+. To allow qualitatively for this effect, we take as an upper limit for the Tl^+ splitting in the crystal the value 1.84 eV of the free ion Tl^{++} splitting. We recognize, of course, that the normalization correction is reduced by increasing the lattice constant of the host crystal (e.g., NaCl, KCl, RbCl). This reduction is neglected in the following discussion.

The other contributions to $\bar{\lambda}$ come from the nn (nearest-neighbor) halides and the nnn (next-nearest-neighbor) alkalis. We assume (and document below) that the nn contribution is negative. Because the spin-orbit interaction is large only near each atomic nucleus, we write the wave function as a linear combination of atomic orbitals and neglect overlap between different atomic sites. It can be shown that in most cases the nnn alkalis' contribution to $\bar{\lambda}$ is negligible. Let α^2 denote the fraction of the impurity wave function on the Tl impurity center, β^2 the fraction on all nn halides in the p state. We take

$$\alpha^2+\beta^2=1 \tag{2.2}$$

and discuss the spin-orbit splitting

$$\bar{\lambda}=\alpha^2\lambda_T-\beta^2\lambda_-. \tag{2.3}$$

We use for λ_- the free halide splittings (Cl, 0.1 eV; Br, 0.4 eV, I, 0.9 eV). Probably λ_T is closer to 1.8 eV than 1.25 eV. The overlap β^2 is proportional to $p_\sigma{}^2$; note that p_σ overlap integrals may reverse sign as a function of Tl^+-halide separation in the region of lattice constants covered by the crystals listed in Table I.

There are two points which emerge from Table I and (2.3). With $\lambda_T=1.84$ eV and $\bar{\beta}^2\sim 0.3$ one obtains first $\bar{\lambda}=1.25$ eV in the chlorides, 1.15 eV in the bromides, and 1.05 eV in the iodides. The averages for the fcc {Na, K, and Rb} salts are 1.37, 1.10, and 0.93, respectively, for chlorides, bromides, and iodides. If one allows for increasing covalency by guessing that β^2 is 0.25, 0.30, 0.35 for chlorides, bromides, and iodides, good agreement with experiment (see Table I) is obtained. Secondly, the trends within the chlorides increase β^2 with increasing lattice constant, whereas the opposite trend obtains within the bromides and iodides. This second point can be explained by assuming that p_σ reverses sign[9] in the chlorides compared to the bromides and iodides.

From the foregoing semiquantitative discussion we see that the sign reversal between (2.1), which holds for covalent crystals, and (2.3), which holds for ionic crystals, is supported by impurity spectra. Other examples which support (2.3) are the inversion of the spin-orbit split exciton levels in ZnO[10] and CuCl.[11] Also sign reversal is indicated by the inverted $2p(\frac{3}{2},\frac{1}{2})$ levels of electrons at F centers in KCl.[12]

The possibility of sign reversal because of closed shell effects is mentioned by Knox[8] and has been treated within a molecular orbital framework by Kamimura.[13] Obviously configuration interaction is involved. One may carry out the usual wave-packet treatment of excitons and impurity states if the interaction is treated as follows. Assume a ground-state wave function of the form (e.g., for an alkali halide)

$$|\Psi_0\rangle=\sum_n \{\alpha|p_-{}^6(\mathbf{r}-\mathbf{R}_n)\rangle+\beta|p_-{}^5(\mathbf{r}-\mathbf{R}_n)p_+\rangle\}, \tag{2.4}$$

where p_- is a halide p orbital and p_+ is an alkali p orbital. Then a hole Bloch state is given by

$$\frac{1}{N}\sum_n e^{i\mathbf{k}\cdot\mathbf{R}_n}a(\mathbf{R}_n)|\Psi_0\rangle, \tag{2.5}$$

where $a(R_n)$ is an electron destruction operator if $\mathbf{r}$ is in the nth cell, zero otherwise. The wave packet obtained from (2.5) contains two kinds of terms: $|p_-{}^5\rangle$ and $|p_-{}^4p_+\rangle$. The contribution to $\bar{\lambda}$ of $p_-{}^5$ is opposite in sign to that of p_+, which is the effect discussed by Knox[8] and Kamimura.[13] Of course, other configurations may also play a role, but the foregoing discussion suggests that some aspects of configuration interaction may be treated within the quasiparticle framework.

We now turn to the Cs halides specifically. Eby, Teegarden, and Dutton[7] have stressed the importance of configuration interaction in these crystals. We discuss here the spin-orbit splitting of the halogen doublet Γ excitons; the extra excitons are discussed in Sec. 6.

The halogen doublet energies are 6.80 and 7.10 eV in CsBr, 5.76 and 5.91 eV in CsI. The splitting in the bromide is 25% smaller than expected from free bromide atom splittings, in the iodide only $\frac{1}{6}$ of that ex-

[9] R. S. Mulliken, C. Rieke, D. Orloff, and H. Orloff, J. Chem. Phys. **17**, 1248 (1949).
[10] D. G. Thomas, Phys. Chem. Solids **15**, 93 (1960).
[11] M. Cardona, Phys. Rev. **129**, 69 (1963).
[12] F. Luty and J. Mort, Phys. Rev. Letters **12**, 45 (1964).
[13] H. Kamimura (to be published).

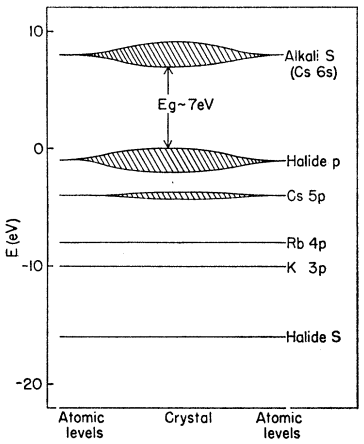

FIG. 1. A sketch of valence and conduction levels in the alkali halides. The position of the alkali core p levels relative to the halide valence band is inferred from free-atom spectra. Note the proximity of the Cs $5p$ levels to the halide p valence band.

pected. Thus our mechanism of configuration interaction must qualitatively be much larger for the iodide.

At first it might appear that interference of the sort (2.3) using electron transfer to the Cs $6p$ state would explain the differences between the Cs salts and the other alkalis. However, the value of $\lambda_{6p}(\mathrm{Cs})$ is only 0.07 eV. To use (2.3) it is necessary to introduce configuration interaction with the Cs core: $\lambda_{5p}(\mathrm{Cs})=1.2$ eV.

To make such configuration interaction appear plausible we show in Fig. 1 a rather old-fashioned sketch of the energy levels of the K, Rb, and Cs halides. In order to avoid Coulomb corrections we have used the neutral free atom term values for, e.g., $5p^6 6s \rightarrow 5p^5 6s^2(\mathrm{Cs})$, to place the alkali p-core levels ($5p$ in Cs). Note that the K $3p$ and Rb $4p$ core levels are well separated from the halide p valence bands, but that the Cs $5p$ valence bands are only a few electron volts below the top of the valence band.

Fermi pointed out[14] that the Cs doublet spectra show strong configuration mixing due to the spin-orbit interaction. Configuration mixing of the Cs $5p$ levels and the halide p levels may be quite large, especially for CsI, where it is facilitated by the large spin-orbit interaction of I. Configuration interaction to distort the orbital bands is presumably much smaller and may be neglected in determining the shape of the valence band in the following section.

3. VALENCE BANDS

No complete calculations are available at present of either the valence or conduction bands of the cesium halides, where the Bravais lattice is simple cubic. The valence bands of fcc KCl have been studied by Howland[15] using the tight-binding method. He has shown that the shape of the top valence bands can be described well in terms of the three halide atomic orbitals (npx, npy, npz) with, e.g., $n=3$ for the chlorides. The actual bandwidth is two times smaller than one would obtain using only these basis functions. This means that the nn $(pp\sigma)$ and $(pp\pi)$ overlap integrals must be renormalized in the spirit of Slater and Koster.[16]

We can construct the valence bands of the Cs halides by taking over the $(pp\sigma)$ and $(pp\pi)$ integrals from Howland's calculation and interpreting them in terms of a simple cubic halide lattice. We must be careful to note that the chloride-chloride distance in CsCl is 4.11 Å, while in KCl it is 4.35 Å. This means that our renormalized overlap integrals should be taken from the valence bands of KCl at lattice constant a 6% smaller than equilibrium a_0. Fortunately Howland gives the valence bands as a function of lattice constant. One finds for $0.90 \leq a/a_0 \leq 0.94$ that

$$(pp\sigma)=0.17\pm0.02 \text{ eV}, \tag{3.1}$$

$$(pp\pi)=-0.08\pm0.02 \text{ eV}. \tag{3.2}$$

Using Table III of Slater and Koster and (3.1) and (3.2), one can construct the p valence bands. The maximum band width is at X and is given theoretically by

$$X_{5'}-X_{1'}=B_t=4(pp\sigma)-4(pp\pi)=1.0 \text{ eV}. \tag{3.3}$$

4. CONDUCTION BANDS

To sketch the conduction bands of the Cs halides we draw on the discussion for the fcc alkali halides and solid rare gases. We noted the importance of d bands, which we expect to be even greater in the Cs halides, in accordance with the trends of the alkali metals.[17]

The energy bands of sc or fcc arrays of square wells have been studied by Pincherle and Lee.[18] Although this model is not a realistic one, it can be used to simulate the conduction bands of interest to us. Contrasting the results for the fcc array with those of the simple cubic, we note:

(1) In the simple cubic lattice the Γ_{12} levels are lower than $\Gamma_{25'}$, whereas the converse holds for the fcc array.

(2) Depending on the well depth the lowest conduction band may be nearly free electron or quite flat. The order of levels is always $\Gamma_1 X_1 M_1 R_1$.

(3) The lowest d band levels may be X_2, M_3, Γ_{12}. This conclusion is tentative and must await, e.g., augmented plane wave studies similar to that of Mattheiss[5] on Ar, for confirmation.

In view of the uncertainties in the ordering of d levels our analysis of the interband spectra will stress transitions between the halide valence bands and the lowest conduction band. When calculations of Cs halide

[14] E. Fermi, Z. Physik **59**, 680 (1929); also see E. U. Condon and G. Shortley, *Theory of Atomic Spectra* (Cambridge University Press, New York, 1953).
[15] L. P. Howland, Phys. Rev. **109**, 1927 (1958).
[16] J. C. Slater and G. F. Koster, Phys. Rev. **94**, 1498 (1954).
[17] F. S. Ham, Phys. Rev. **128**, 82, 2524 (1962).
[18] L. Pincherle and P. M. Lee, Proc. Phys. Soc. (London) **78**, 1195 (1961).

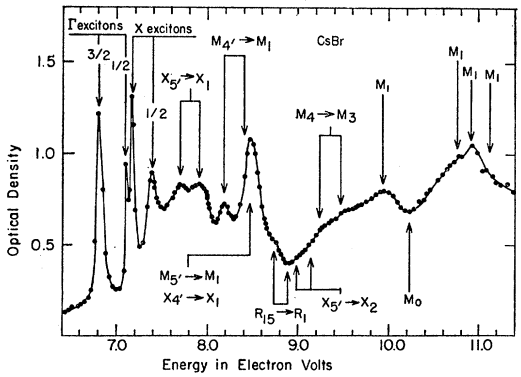

FIG. 2. Optical transmission of CsBr films at 80°K. The experimental data are taken from Ref. 7, while the theoretical interpretation is given in the text.

conduction bands are available it should be feasible to extend our analysis to include higher conduction bands.

5. INTERBAND SPECTRA

The analysis of interband spectra is facilitated by large spin-orbit splittings. Because of configuration interaction[7] it appears that CsBr with $\lambda=0.2$ eV is the most favorable case. The general features deduced from its spectrum will contribute to the analysis of CsCl and CsI.

To carry out our analysis we begin by sketching the valence and conduction bands according to the considerations of Secs. 3 and 4. With slight modifications these bands were found to account qualitatively for the experimental results as indicated in Fig. 2. The energy bands are shown in Fig. 3.

We have not been able to identify the direct energy gap $\Gamma_{15}(\frac{3}{2}) \rightarrow \Gamma_1$. It seems to be hidden beneath the extra exciton at 7.18 eV. It seems likely that the $\Gamma_{15}(\frac{1}{2}) \rightarrow \Gamma_1$ threshold occurs at 7.45 eV, although it is obscured by the extra exciton at 7.39 eV.

The interband spectrum may be broadly divided into two parts:

$$S: \quad 7.2 \text{ eV} \leq E \leq 8.9 \text{ eV}, \tag{5.1}$$

$$D: \quad 9.0 \text{ eV} \leq E \cdots. \tag{5.2}$$

The S part corresponds to transitions from the valence band to the conduction band states $\Gamma_1 X_1 M_1 R_1$. The D part represents transitions from the valence band to d-band states such as Γ_{12} and $\Gamma_{25'}$. We do not know its upper limit, although it certainly extends to 11 eV. According to Fig. 1, beyond 11 eV Cs $5p \rightarrow$ Cs$6s$ (conduction band) transitions should be prominent. Reflectance studies of the spectrum beyond 11 eV would be of considerable interest.

Note that near 9.0 eV the optical density is low. We believe that, neglecting lifetime effects, the interband scattering spectrum would be transparent between 8.9 and 9.0 eV.

Because the conduction band width is substantially greater than the valence bandwidth analysis of the rather complicated S spectrum is not difficult. The first two peaks at 7.68 and 7.90 eV are certainly due to the spin-orbit split transition $X_{5'} \rightarrow X_1$. The first peak of $M_{4'} \rightarrow M_1$ is seen at 8.17 eV, but the second is buried under the strong peak of 8.46 eV. This "Lorentzian" peak probably represents the accidental confluence of lifetime broadened edges of types M_1 and M_2, as shown in Table I. The $R_{15} \rightarrow R_1$ transitions mark the end of the S spectrum.

Interpretation of the D spectrum must await a complete band calculation. We have recognized many Van Hove edges which are marked in Fig. 2. The lowest three or four are tentatively identified and listed in Table II.

TABLE II. Interband exciton and scattering structure in eV. The features which are marked in Figs. 2 and 4 are tabulated with an accuracy of ±0.02 eV.

			CsBr	CsCl (sc)
Excitons				
	$\mathbf{k}_0$	$J(m_J)$		
	Γ	$\frac{3}{2}$	6.80	7.80
	Γ	$\frac{1}{2}$	7.10	7.91
	X	$\frac{3}{2}$	7.18	8.00
	X	$\frac{1}{2}$	7.38	8.11
Scattering spectra				
	$(\mathbf{k},n)$	$J(m_J)$	CsBr	CsCl (sc)
S	$X_5' \rightarrow X_1$	$\frac{3}{2}$	7.69	8.48
		$\frac{1}{2}$	7.91	8.61
	$M_4' \rightarrow M_1$	$\frac{3}{2}$	8.18	8.74
		$\frac{1}{2}$		8.83
	$M_5' \rightarrow M_1$		8.44	9.10
	$X_4' \rightarrow X_1$		8.44	9.10
	$R_{15} \rightarrow R_1$	$\frac{3}{2}$	8.72	9.34
		$\frac{1}{2}$	8.88	9.44
D	$X_5' \rightarrow X_2$	$\frac{3}{2}$	8.96	9.58
		$\frac{1}{2}$	9.16	9.74
	$M_4' \rightarrow M_3$	$\frac{3}{2}$	9.22	
		$\frac{1}{2}$	9.44	

From our discussion of the S spectrum we can estimate the orbital width of the valence band, from the

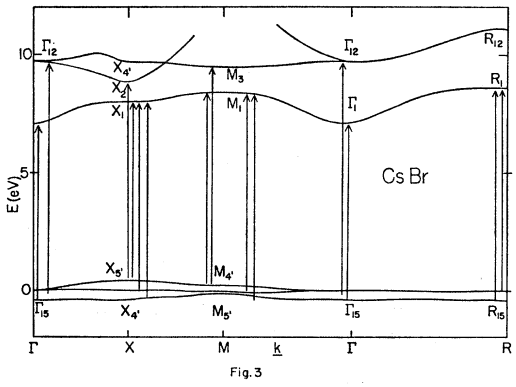

FIG. 3. The energy bands of CsBr as inferred by combining the discussion of Secs. 3 and 4 with the interband scattering spectra identified in Fig. 2 and listed in Table II.

center of gravity of $X_{5'}$ to $X_{4'}$. This turns out to be

$$B_{\text{exp}}=0.67\pm0.05 \text{ eV}. \quad (5.3)$$

By comparing this with (3.3) we see that the observed band width is about $\frac{2}{3}$ the value predicted by Howland's tight-binding calculations.[15] This result is in satisfying agreement with Howland's observation that expanding his basis set from 3 to 8 atomic orbitals reduced the bandwidth by a factor of 2. A complete basis set might well lead to the renormalized bandwidth (5.3). This reduction in orbital bandwidth is qualitatively similar to the "compressive" increase in spin-orbit splitting discussed in Sec. 2. This completes our discussion of CsBr scattering spectra.

Normally CsCl crystallizes in a simple cubic lattice (called II by ETD), but one can attempt by epitaxial deposition to prepare it in the fcc form (I). We begin with the sc spectrum shown in Fig. 4. Analysis of this spectrum proceeds along lines similar to that for CsBr. The gap between the S and D spectra falls at 9.5 eV. The value of λ ($\sim$0.1 eV) is too small to render spin-orbit splittings in the scattering spectra resolvable. Consequently identification of structure in the S spectrum is less reliable. Nevertheless the over-all similarity between the S spectra of CsBr and CsCl is evident. The energy bands of CsCl can be constructed by analogy with Fig. 3 using the interband energy differences shown in Table II.

The scattering spectrum of CsI shown in Fig. 5 is dissimilar to the spectra of CsBr and CsCl. We believe this change is caused by the lowering of the d conduction band levels by the iodide ions. This in turn results in overlapping S-D spectra as well as a general distortion of the lowest conduction band as sketched in Fig. 3. It is possible (though less likely) that the iodide ions introduce appreciable $4f$ character into the conduction band levels.

Perhaps because of overlap with the D spectrum only one scattering peak near 6.8 eV is seen at low energies in CsI. In general, room-temperature spectra are merely

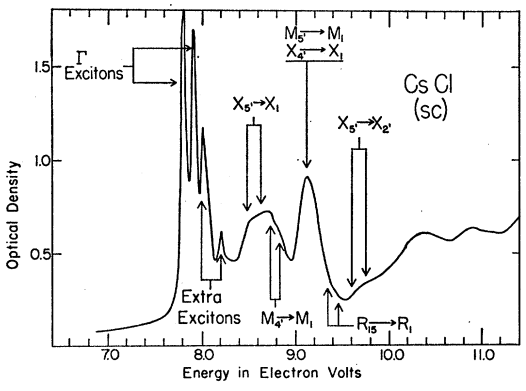

FIG. 4. Optical transmission through simple cubic CsCl films at 80°K. The experimental data are taken from Ref. 7, while the theoretical interpretation is given in the text.

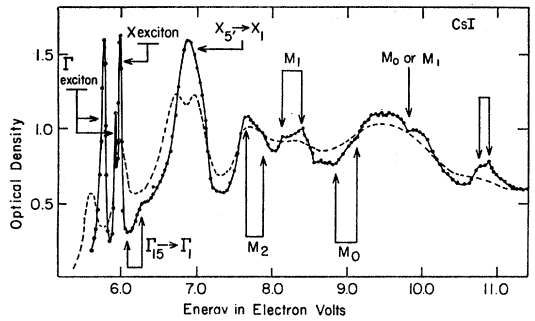

FIG. 5. Optical transmission through CsI films. The experimental points are taken from Ref. 7, and refer to 80°K. The dashed line refers to room temperature.

broadened versions of low-temperature spectra and are generally omitted from our figures for that reason. However, the room-temperature CsI spectrum also shown in Fig. 5 taken by ETD shows a doublet structure near 6.8 eV which is absent at 80°K. Although the presence of extra structure at higher temperatures is difficult to understand, it may be indicative of an $X_{5'} \rightarrow X_1$ spin-orbit split transition. (See note added in manuscript.)

At higher energies (where the S-D spectra may overlap) several pairs of Van Hove singularities are resolved. We have a pair of type M_2 at 7.70 and 7.92 eV; a pair of type M_1 at 8.14 and 8.40 eV, and a pair of type M_0 at 8.88 and 9.16 eV. The separation of each pair is about 0.25±0.03 eV, which suggests that they are associated with spin-orbit splitting of the valence band. The spin-orbit splitting of the Γ excitons is only 0.15 eV. Presumably the difference arises from configuration interactions of the Γ excitons with X excitons.[4]

We conclude by discussing the scattering spectrum of epitaxial CsCl films, which seem to be mixed fcc and sc (see Fig. 6). The peaks near 8.7 and 9.2 eV correspond to stronger peaks in the sc spectrum at the same energies. The very strong, rather narrow peak at 11.0 eV, on the other hand, is not present in the sc spectrum. The line shape is similar (but rather more narrow) to the $X_{5'} \rightarrow X_1$ structure seen in fcc crystals. It is evident that resonant scattering of a peculiar kind must be taking place in the mixed crystal.

6. EXCITON SPECTRA

Again to minimize the effects of configuration interaction we begin with the excitons in CsBr. As shown in Table II the splitting of the halogen doublet Γ excitons is 0.30 eV, while the X excitons (with parent interband edges $X_{5'} \rightarrow X_1$ split by 0.22 eV) are split by 0.20 eV. Because the $X_{5'}$ level is twofold degenerate compared to the threefold degeneracy of Γ_{15}, a splitting ratio $X/\Gamma=\frac{2}{3}$ is expected and observed. Thus the extra ex-

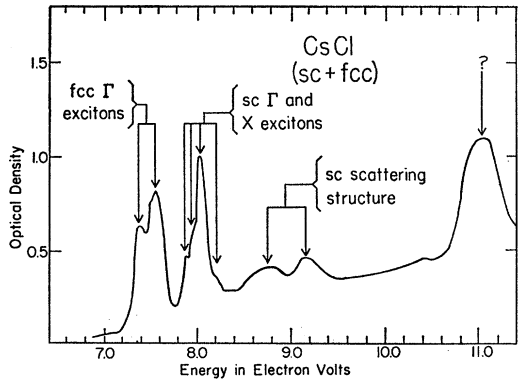

FIG. 6. Optical transmission through CsCl films at 80°K. The films were grown epitaxially on an fcc substrate. For reasons discussed in the text we believe the films represent mixed sc and fcc crystalites.

citons in CsBr are of the same type as the extra[19] metastable L excitons[3,4] in the fcc alkali halides.[20,21]

In CsCl the extra excitons show (see Table II) the same spin-orbit splitting of 0.11 eV as the Γ excitons. Because the splitting is so small the failure of the $\frac{2}{3}$ rule may not be significant. It is possible, e.g., that the position of the $X(m_J=\frac{3}{2})$ peak at 8.00 eV has been shifted from 8.03 eV because of overlap or configuration interaction with the stronger $\Gamma(\frac{1}{2})$ peak at 7.91 eV.

The CsI spectrum shows the halogen doublet at 5.76 and 5.91 eV. Also the $\Gamma_{15}(\frac{3}{2}) \rightarrow \Gamma_1$ threshold is located at 6.28 eV. (Most of the oscillator strength of the threshold seems to have been transferred to the excitons, with a resulting change in threshold line shape.) As we have mentioned in Sec. 4, this small exciton splitting is probably attributable partly to configuration interaction between Cs $5p$ and I $5p$ levels mediated by the spin-orbit operator and partly to interaction with the X excitons.

There is only one extra excition in CsI, located at 5.97 eV. We identify this as the $X(\frac{3}{2})$ exciton. The absence of the $X(\frac{1}{2})$ exciton which should fall near 6.1 eV can be attributed to autoionization. The $X(\frac{1}{2})$ exciton is metastable in CsBr and CsCl, but not in CsI. The halide-halide overlap in the iodide is greater than in the bromide or chloride. This inhibits exciton self-trapping through hole-lattice interactions. Thus, if we wished, we could account for the absence of the $X(\frac{1}{2})$ excitons as a failure of the same Jahn-Teller distortion postulated in III to account for the absence of metastable excitons in some fcc alkali halides.

It seems to us, however, that the electron-electron interactions which are responsible for the reduction in spin-orbit splitting in CsI probably play an equally important role in delocalizing the hole in the valence band. If the latter contains in addition to the $5p$ iodide orbitals a substantial admixture of Cs $5p$ orbitals, self-trapping of the hole at an I_2^- molecule would be inhibited. Thus the $X(\frac{3}{2})$ exciton survives only because it does not overlap the scattering continuum at all. The predicted position of the $X(\frac{1}{2})$ exciton is near 6.10 eV, where the interband scattering spectrum is weak. Nevertheless rapid autoionization takes place, not primarily because of electron-phonon interactions, but because of electron-electron interactions.

7. CONCLUSIONS

We have seen that considerable progress can be made in understanding the spectra of the Cs halides in spite of the obstacles discussed in the introduction. We have provided tentative constructions of the energy bands of these crystals. It is to be hoped that using modern computational methods these can be confirmed at low energies. It should then be possible to extend the analysis into the conduction d-band region.

Further experimental work should probably aim at completing the spectra by carrying out high-energy reflectance studies. One might hope thereby to shed light on the (Cs $5p$)-(I $5p$) mixing discussed in Secs. 4 and 6. It might also be feasible to obtain ϵ_2 (instead of the absorptivity) by polarization studies or Kramers-Kronig transforms.[22] The line shape in ϵ_2 is more readily interpretable than the line shape of optical density of films studied by ETD.

Should more perfect alkali halide bulk crystals become available it would be extremely interesting to study metastable exciton line shapes by the polarimetry reflectance method at 20°K. It is possible that using the best crystals now available further insight could be obtained, bearing in mind the interference between exciton and interband scattering which has been discussed elsewhere.[23,4]

Note added in manuscript. Several interesting models based on atomic orbitals or crystalline levels only at $\mathbf{k}=0$ have been proposed to account for the spectra of the Cs halides. For CsI there is the experimental and theoretical work (atomic orbitals) of Fischer and Hilsch.[24] Similar remarks for the other Cs halides have been made (using crystalline levels only at $\mathbf{k}=0$) by Knox.[25] Because the Fischer and Hilsch work on CsI is more complete, we discuss it in detail. Most of our general remarks also apply to Knox's model.

Fischer and Hilsch explain the splitting of the peak near 6.8 eV at high temperatures as the shift of a lower peak downwards to 6.6 eV on going from $T=0$ to 400°K while an upper peak (perhaps a doublet) shifts slightly upwards to 6.9 and 7.0 eV. On our model these shifts

[19] We use the phrase "extra excitons" to describe excitons which are not of the conventional hydrogenic type, but are derived from interband saddle-point edges of Van Hove type M_1.

[20] Our previous statement (Ref. 21) concerning the multiplicity of extra excitons in the Cs halides is in error and should be disregarded.

[21] J. C. Phillips, Phys. Rev. Letters **12**, 142 (1964).

[22] H. R. Phillipp and E. A. Taft, Phys. Rev. **113**, 1002 (1959).

[23] J. C. Phillips, Phys. Rev. Letters **12**, 447 (1964).

[24] F. Fischer and R. Hilsch, Z. Physik **158**, 553 (1960); **160**, 194 (1960); Nachr. Akad. Wiss. Gottingen **8**, 241 (1959).

[25] R. Knox, Phys. Rev. **133**, A498 (1964).

are readily understood in terms of the valence band structure shown in Fig. 3 for CsBr (the valence band structure of CsI is similar, but with smaller spin-orbit splittings). We discuss the temperature dependence of valence band states because the coupling of these states to the lattice may be stronger than that of the nearly free electron conduction band. Then $X_{5'}$ (which is near the top of the valence band) should shift strongly upward with temperature, by about the same amount as the $\Gamma_{15}(\frac{3}{2})$ exciton, as observed. On the other hand, $M_{4'}$ lies close to the center of the p valence band and its temperature dependence should be small (cf., the second-order perturbation theory of temperature dependence of interband edges in semiconductors).

We now identify the lower peak with $X_{5'} \rightarrow X_1$, the upper peaks with $M_{4'} \rightarrow M_1$. This explains qualitatively the observed temperature dependence.

Fischer and Hilsch suggest that the lower peak may be the $\Gamma(\frac{1}{2})$ exciton, while the doublet at 5.91 and 5.97 eV is associated with atomic orbitals of the Cs $6p$ type. Their model is weak both (a) phenomenologically and (b) theoretically.

(a) As expected from the multiplicity of the valence band edges, the oscillator strength of the $\Gamma(\frac{3}{2})$ exciton should be about twice that of the $\Gamma(\frac{1}{2})$ exciton. This is found to be the case for the halogen doublet in the fcc alkali halides (KBr is a good example). If we accept the Fischer-Hilsch model, the oscillator strength of the "$\Gamma(\frac{1}{2})$ exciton" at 6.6 eV is about four times that of the $\Gamma(\frac{3}{2})$ exciton, or about 8 times greater than it should be.

(b) According to our theoretical band model, the Cs $6p$ states in the conduction band must occur 3 or 4 eV higher than the Cs $6s$ states. It follows that such states play no significant role in determining exciton structure near 6.0 eV. Moreover, interband transitions $\Gamma_{15} \rightarrow \Gamma_{15}$ are dipole forbidden.

It has been suggested that the peculiar behavior of the 5.91, 5.97 eV doublet in CsI can be explained by assuming that the doublet is derived from X excitons. This suggestion has several attractive features:

(A1) The small splitting of 0.06 eV can be ascribed to the splitting of $X_{5'}$ rather than Γ_{15}.

(A2) The temperature stability of the splitting (see Fischer and Hilsch) follows from the assignment of both excitons to the X region.

Unfortunately the suggestion also suffers from several fata defects:

(B1) Where do we put the $\Gamma(\frac{1}{2})$ exciton?

(B2) In general, for Γ_{15}, $X_{5'}$, and $L_{3'}$, the higher energy hole has the heavier mass. This means that the lower energy exciton of a spin-orbit split doublet always has the greater oscillator strength (e.g., CsBr). But in this case the 5.97-eV exciton is stronger.

One may resolve (B1) and (B2) by assuming that the $\Gamma(\frac{1}{2})$ and higher X exciton are degenerate, with no configuration interaction to repel them from each other. This is implausible on the face of it. It also leads to a splitting ratio $X/\Gamma=0.3$, which is much smaller than the value of $\frac{2}{3}$ found in CsBr.

The common impulse to assign both doublet peaks to the same region of the Brillouin zone is based on the remarkable temperature independence of the splitting described by Fischer and Hilsch. Equally remarkable, however, is the temperature independence of the center of gravity of these excitons. According to second-order perturbation theory, with increasing temperature an exciton resonance should move to lower (higher) energies if the center of gravity of the virtual intermediate states (to which it scatters by phonon emission or absorption) is above (below) the resonance (see Table I of paper IV).

The only oscillator strength below the doublet is that of the $\Gamma(\frac{3}{2})$ exciton. This means that at least one of the doublet peaks must couple as strongly to the $\Gamma(\frac{3}{2})$ exciton as it does to all other states combined. With the optical phonon coupling proportional to q^{-2} (where $q=\mathbf{k}-\mathbf{k}'$ is the phonon momentum) this is possible only if one of the peaks is actually the $\Gamma(\frac{1}{2})$ exciton. Because of (B2) we have assigned the $\Gamma(\frac{1}{2})$ exciton to 5.91 eV and the lower X exciton to 5.97 eV. The higher X exciton is not observable in the spectrum because of lifetime effects.

It is clear that the temperature independence of the center of gravity of the doublet is somewhat accidental. However, the temperature independence of the splitting need not be accidental. We believe that the 0.06-eV splitting is caused by configuration repulsion between the $\Gamma(\frac{1}{2})$ exciton and both X excitons. (For configuration interaction to occur between two resonances it is not necessary for both to be resolved in the spectrum; it is only necessary that the linewidths be small compared to the spacing of the resonances.)

From the foregoing discussion it is clear that the exciton structure in CsI is complex, as mentioned in the introduction. This should not be allowed to distract the reader from our central conclusion, which is the following:

Models which discuss levels only near $\mathbf{k}=0$ omit about 90% of the oscillator strength which contributes to the fundamental absorption spectrum. Such models can describe at most only the halogen doublet structure, and are not appropriate to most of the fundamental absorption region. In many cases inclusion of saddle-point excitons from regions of $\mathbf{k}$ space other than Γ completely explains both the extra resonances and broad, high-energy peaks.